Available online at www.sciencedirect.com
ScienceDirect
Journal of Organometallic Chemistry 692 (2007) 5007–5016
Journal of Organometallic Chemistry
www.elsevier.com/locate/jorganchem

Two modes of C–H bond activation of tris(2-thienyl)phosphine in trinuclear osmium carbonyl clusters

M. Abdul Mottalib [a], Shariff E. Kabir [b,c,*], Derek A. Tocher [c], Antony J. Deeming [c], Ebbe Nordlander [a,*]

[a] *Inorganic Chemistry Research Group, Chemical Physics, Center for Chemistry and Chemical Engineering, Lund University, P.O. Box 124, SE-22100 Lund, Sweden*
[b] *Department of Chemistry, Jahangirnagar University, Savar, Dhaka, Bangladesh*
[c] *Department of Chemistry, University College London, 20 Gordon Street, London WC1H 0AJ, United Kingdom*

Received 6 June 2007; received in revised form 18 July 2007; accepted 19 July 2007
Available online 2 August 2007

Abstract

Tris(2-thienyl)phosphine, $P(C_4H_3S)_3$, reacts with $[Os_3(CO)_{12}]$ at 110 °C to give the phosphine-substituted derivatives $[Os_3(CO)_{11}\{P(C_4H_3S)_3\}]$ (**1**), $[Os_3(CO)_{10}\{P(C_4H_3S)_3\}_2]$ (**2**) and $[Os_3(CO)_9\{P(C_4H_3S)_3\}_3]$ (**4**), as well as the C–H activated product $[Os_3(\mu\text{-}H)(CO)_9\{\mu\text{-}P(C_4H_2S)(C_4H_3S)_2\}\{P(C_4H_3S)_3\}]$ (**3**), in which the bridging ligand is equatorially coordinated to two osmium atoms. Thermolysis of **2** in refluxing toluene results in the formation of **3**. Compound **1** can also be prepared in high yield from $[Os_3(CO)_{11}(NCMe)]$. The reaction of $[Os_3(\mu\text{-}H)_2(CO)_{10}]$ with tris(2-thienyl)phosphine at room temperature afforded $[Os_3(\mu\text{-}H)_2(CO)_9\{P(C_4H_3S)_3\}]$ (**5**) and $[Os_3H(\mu\text{-}H)(CO)_{10}\{P(C_4H_3S)_3\}]$ (**6**), with the ligand coordinated through the phosphorus atom whereas at elevated temperature the cyclometallated compounds $[Os_3(\mu\text{-}H)(CO)_9\{\mu_3\text{-}P(C_4H_2S)(C_4H_3S)_2\}]$ (**7**) and $[Os_3(\mu\text{-}H)(CO)_8\{\mu_3\text{-}P(C_4H_2S)(C_4H_3S)_2\{P(C_4H_3S)_3\}]$ (**8**) were obtained in addition to **5**. Heating **6** in refluxing heptane furnished **5** via loss of one carbonyl ligand. Thermolysis of **1** and **3** in refluxing toluene gives **7** and **8**, respectively, in good yields. In **3**, the $\mu\text{-}P(C_4H_2S)(C_4H_3S)_2$ ligand is coordinated through the phosphorus to one Os atom and through a σ–Os–C bond to the second osmium atom. Compound **7** contains the $\mu_3\text{-}P(C_4H_2S)(C_4H_3S)_2$ ligand bound through phosphorus to one Os atom, through a σ–Os–C bond to another and by an η^2 (π)-interaction to the third osmium atom. Compounds **1**, **2** and **4** contain the ligand coordinated exclusively through the phosphorus atom. The crystal and molecular structures of **2**, **3**, **5**, **6** and **7** are reported.

Keywords: Triosmium clusters; Tris(2-thienyl)phosphine; Cyclometallation

1. Introduction

The reactions of thiophene and its benzo-derivatives with metal carbonyl clusters have been investigated in efforts to model hydrodesulfurization processes, which involve the removal of thiophenic sulfur from crude oil [1]. One of the earliest reports of the interaction of thiophene with organometallic compounds described the desulfurization of the heterocycle by $[Fe_3(CO)_{12}]$ [2,3]. Rauchfuss and coworkers [4] demonstrated that thiaferroles are easily converted to the corresponding ferroles and they established that insertion of an iron atom into a C–S bond clearly activates the heterocycle towards desulfurization. The reaction of $[Ru_3(CO)_{12}]$ with thiophene proceeds similarly via C–S cleavage giving $[Ru_2(\mu\text{-}C_4H_4)(CO)_6]$ and $[Ru_4(\mu_3\text{-}S)(\mu\text{-}C_4H_4)(CO)_{11}]$ [5]. It has been demonstrated that C–H bond activation predominates over C–S cleavage when thiophene reacts with $[Os_3(CO)_{12}]$ and $[Os_3(CO)_{10}(MeCN)_2]$ yielding $[Os_3(\mu\text{-}H)(\mu\text{-}C_4H_2S)(CO)_9]$ [6]. The C–S bond cleavage of

* Corresponding authors. Fax: +46 46 222 4119 (E. Nordlander).
E-mail addresses: Skabir_ju@yahoo.com (S.E. Kabir), Ebbe.Nordlander@inorg.lu.se (E. Nordlander).

0022-328X/$ - see front matter © 2007 Elsevier B.V. All rights reserved.
doi:10.1016/j.jorganchem.2007.07.042

benzothiophene when coordinated to a triosmium cluster $[Os_3(\mu_3\text{-}S)(\mu\text{-}C_8H_5S)(CO)_{10}]$ has been reported to give $[Os_3(\mu\text{-}C_8H_6S)(CO)_{10}]$ which contains an open benzothiophene ligand coordinated to an open Os_3 unit through a μ-S and μ-η^2-vinyl group [7,8].

Despite the above examples of coordination and activation, thiophene and its benzo-derivatives are relatively poor ligands for low-valent transition metals, and phosphothiophenes such as diphenyl-2-thienylphosphine have therefore been used as a route to thienyl ligands [9–11]. We have shown that the reaction of diphenyl-2-thienylphosphine with $[Ru_3(CO)_{12}]$ gives $[Ru_3(\mu\text{-}H)(\mu_3\text{-}Ph_2PC_4H_2S)(CO)_9]$, $[Ru_3(\mu\text{-}H)(\mu_3\text{-}Ph_2PC_4H_2S)(CO)_8(Ph_2PC_4H_3S)]$, $[Ru_4(\mu_4\text{-}PPh)(\mu_4\text{-}C_4H_4)(CO)_{11}]$ and $[Ru_4(\mu_4\text{-}PPh)(\mu_4\text{-}C_4H_2S)(CO)_{11}]$ via cyclometallation and P–C bond cleavage of the ligand [11]. In order to compare the reactivities of the ruthenium clusters with their osmium homologues, we have extended this work to triosmium clusters. Thus, we recently reported that $[Os_3(CO)_{12}]$ and $[Os_3(\mu\text{-}H)_2(CO)_{10}]$ react with diphenyl-2-thienylphosphine to give substitution products with the ligand coordinated in mono- and bidentate coordination modes via its phosphorus and sulfur atoms and, in addition, C–H cleavage at the thienyl ring of the ligand [12]. Furthermore, Vahrenkamp et al. [13] have demonstrated that the tris(2-thienyl)phosphine substituted compounds $[Ru_3(CO)_{10}\{P(C_4H_3S)_3\}_2]$ and $[Ru(CO)_3\{P(C_4H_3S)_3\}_2]$ can be prepared from the ketyl initiated reaction between $[Ru_3(CO)_{12}]$ and tris(2-thienyl)phosphine. As a part of our studies of the reactivity of triosmium clusters with phosphothiophenes, we report here the reactions of $[Os_3(CO)_{12}]$ and $[Os_3(\mu\text{-}H)_2(CO)_{10}]$ with tris(2-thienyl)phosphine.

2. Results and discussion

The reaction of $[Os_3(CO)_{12}]$ with tris(2-thienyl)phosphine in refluxing toluene afforded the mono-, di- and triphosphine substituted derivatives $[Os_3(CO)_{11}\{P(C_4H_3S)_3\}]$ (**1**), $[Os_3(CO)_{10}\{P(C_4H_3S)_3\}_2]$ (**2**) and $[Os_3(CO)_9\{P(C_4H_3S)_3\}]$ (**4**) in 28%, 33% and 3% yields, respectively, as well as the C–H activated product $[Os_3(\mu\text{-}H)(CO)_9\{\mu\text{-}P(C_4H_2S)(C_4H_3S)_2\}\{P(C_4H_3S)_3\}]$ (**3**) in 13% yield (Scheme 1). Compound **1** can also be obtained in 80% yield by the treatment of $[Os_3(CO)_{11}(NCMe)]$ with an equimolar amount of the thienyl-phosphine ligand at ambient temperature.

Compounds **1**, **2** and **4** could be identified by comparison of their ν_{CO} IR absorption patterns to those of related mono-, di- and triphosphine-substituted osmium clusters [14]. The mass spectra of all three compounds were also in complete agreement with the proposed formulas. The ^1H NMR spectra of **1**, **2** and **4** exhibit resonances only in the aromatic region. The room temperature $^{31}P\{^1H\}$ NMR spectra show a singlet at δ −32.97 for **1**; a broad signal at δ −44.73 for **2** and a singlet at δ −47.0 for **4**. The broad signal for **2** is indicative of fluxional behaviour, which has also been observed for the analogous disubstituted cluster $[Os_3(CO)_{10}\{Ph_2P(C_4H_3S)\}_2]$ [12]. We [12,15] and others [16] have demonstrated that $[Os_3(CO)_{10}(phosphine)_2]$ clusters exist in solution as mixtures of *trans-trans* and *cis–trans* isomers of which the latter appears to be the thermodynamically favoured isomer that predominates at low temperatures while the two isomers are usually found to be in rapid equilibrium at room temperature. In the case of $[Os_3(CO)_{10}\{Ph_2P(C_4H_3S)\}_2]$ [12], the fluxionality could be frozen out at −60 °C to reveal the existence of two isomers with the *cis–trans* isomer being favoured at low temperature, but the fluxionality was not investigated in detail in the present case. In general, the *trans–trans* isomers crystallize and their structures are well established. The structure of the *trans–trans* isomer of $[Os_3(CO)_{10}(PPh_3)_2]$ was reported by Bruce et al. [17] in 1988, while Leong and Liu [18] have more recently reported the structure of the *cis–trans* isomer, which was the first example of crystallographic identification of such an isomer. Another, more recent, example of the identification of a *cis–trans* isomer is $[Os_3(CO)_{10}\{Ph_2P(C_4H_3S)\}_2]$, which has also been characterized by X-ray crystallography [12].

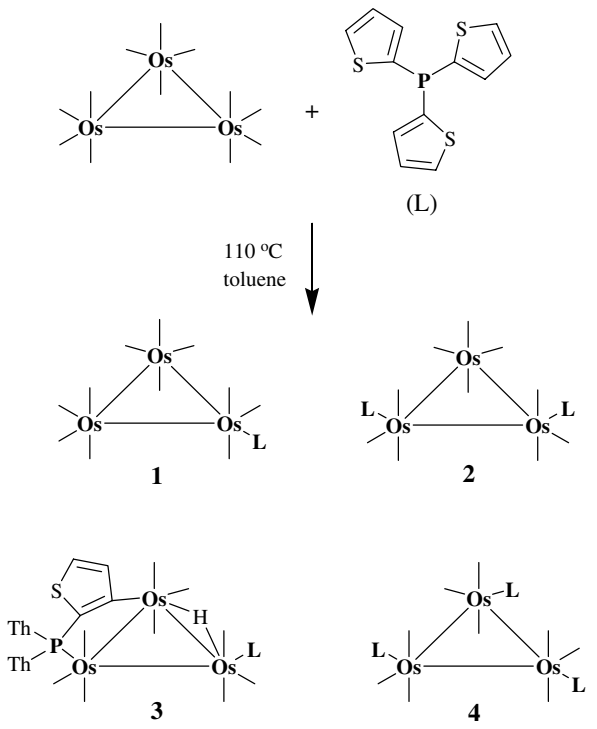

Scheme 1.

In order to confirm whether compound **2** crystallizes in the *trans–trans* or *cis–trans* form, a single crystal X-ray analysis of **2** was undertaken. The molecular structure of **2** is shown in Fig. 1 and relevant crystallographic data are listed in Table 1. The overall structure of **2** is similar to that of *trans–trans* $[Os_3(CO)_{10}(PPh_3)_2]$ [17,18]. The molecule consists of a triangular metal core of osmium atoms with ten terminal carbonyl ligands and two tris(2-thie-

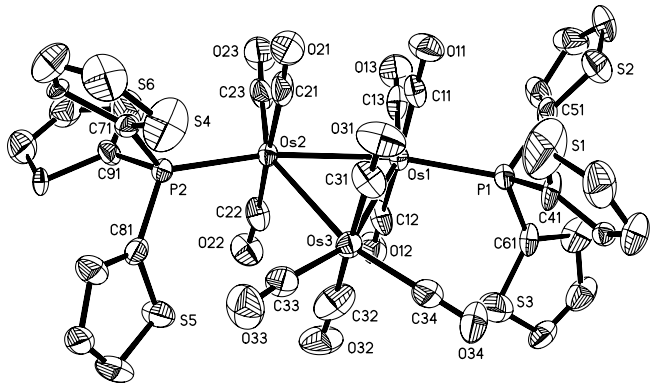

Fig. 1. Solid-state molecular structure of 1,2-$[Os_3(CO)_{10}\{P(C_4H_3S)_3\}_2]$ (**2**). Thermal ellipsoids are drawn at the 50% probability level and the hydrogen atoms have been omitted for the sake of clarity. Selected bond lengths (Å) and angles (°): Os(1)–Os(2) = 2.8829(7), Os(1)–Os(3) = 2.9093(9), Os(2)–Os(3) = 2.9063(8), Os(1)–P(1) = 2.324(3), Os(2)–P(2) = 2.334(3), Os(2)–Os(1)–Os(3) = 60.232(18), Os(1)–Os(2)–Os(3) = 60.334(19), Os(2)–Os(3)–Os(1) = 59.434(18), P(2)–Os(2)–Os(1) = 168.02(8), P(2)–Os(2)–Os(3) = 107.76(8), P(1)–Os(1)–Os(2) = 163.45(9), P(1)–Os(1)–Os(3) = 103.56(9), C(23)–Os(2)–Os(3) = 149.1(5),C(21)–Os(2)–Os(3) = 89.6(5), C(22)–Os(2)–Os(3) = 89.1(5), C(13)–Os(1)–Os(3) = 158.1(5), C(12)–Os(1)–Os(3) = 88.9(5), C(11)–Os(1)–Os(3) = 93.0(4).

nyl)phosphine ligands. The metal–metal bond distances [Os(1)–Os(3) = 2.909(9), Os(2)–Os(3) = 2.906(8) and Os(1)–Os(2) = 2.882(7) Å] are comparable to the corresponding distances in the *trans–trans* isomer of $[Os_3(CO)_{10}(PPh_3)_2]$ [2.9065(4), 2.9095(4) and 2.8988(5) Å]. The two tris(2-thienyl)phosphine ligands are coordinated through the phosphorus atoms in the equatorial sites on adjacent osmium atoms and each of them is *trans* to the phosphine-substituted Os–Os edge as has been reported for related $[Os_3(CO)_{10}(L)_2]$ clusters (L = PPh_3, $PPh(OMe)_2$, and $P(OMe)_3$) [17–19]. The Os–P bond distances [Os(1)–P(1) = 2.324 (3) and Os(2)–P(2) = 2.334(3) Å] are normal and close to those reported for both isomers of $[Os_3(CO)_{10}(PPh_3)_2]$ [2.351(2) and 2.361(2) Å for the *cis–trans* isomer and 2.3607(12) and 2.3478(13) Å for the *trans–trans* isomer] [18].

The infrared spectrum of **3** indicates that all the carbonyl groups are terminal and its pattern is different from those reported for $[Os_3(\mu\text{-H})(CO)_8\{\mu_3\text{-}PPh_2(C_4H_3S)_2\}\text{-}\{PPh_2(C_4H_3S)\}]$ [12] and $[Os_3(\mu\text{-H})(CO)_8\{\mu_3\text{-}PPh_2\text{-}(C_8H_4S)_2\{PPh_2C_8H_4S)\}]$ [20]. Furthermore, the mass spectrum of **3** indicates that it possesses nine rather than eight carbonyls. The ^{1}H NMR spectrum of the cluster shows nine multiplets and two doublets in the aromatic region. The former integrate to 15 protons while the latter two integrate to one proton each and are characteristic of C–H activation of one of the thienyl rings. The hydride region of the ^{1}H NMR spectrum contains a doublet of doublets at δ −17.15 (J = 15.9 and 11.4 Hz), owing to the coupling of one hydride to two non-equivalent ^{31}P nuclei. Consistent with this, the $^{31}P\{^1H\}$ NMR spectrum displays two doublets at δ −33.22 and −34.05 (J = 21.3 Hz).

The crystal structure of **3** was determined by X-ray crystallography and was found to be in agreement with the solution data mentioned above. The solid state molecular structure of **3** is shown in Fig. 2. The molecule consists of an irregular triangular array of osmium atoms with one significantly shorter [Os(1)–Os(2) = 2.856 Å] and two elongated [Os(1)–Os(3) = 2.910 and Os(2)–Os(3) = 3.056 Å] metal–metal bonds, nine terminal carbonyl groups, one orthometallated tris-2-thienylphosphine and one terminal tris-2-thienylphosphine ligand. The orthometalated $P(C_4H_2S)(C_4H_3S)_2$ ligand is coordinated via the phosphorus atom, P(1), occupying an equatorial site on Os(2) and via the thienyl ring to Os(1) through a σ interaction [Os(2)–C(42) = 2.130(14) Å]. Unlike the triply bridging coordination mode that has been observed previously for a number of thienylphosphine ligands [11,12] (*vide infra*), and which involves both σ- and π-coordination of the thienyl ring, the present coordination mode permits the bridging thienylphosphine ligand to coordinate in equatorial coordination sites at both Os(1) and Os(2). This is, to our knowledge, the first example of this type of coordination mode for a thienylphosphine ligand. The orthometallation of the ligand yields a chiral cluster framework [21] but the compound crystallizes as a racemic mixture. The hydride ligand was not located directly, but bridging hydride ligands are known to produce significant lengthening effects on metal-metal bonds, and it is thus possible to predict that the bridging hydride spans the Os(2)–Os(3) edge since this edge is substantially elongated [Os(2)–Os(3) 3.0564(7) Å]. Furthermore, the significant bending away of the phosphine ligand and the equatorial carbonyl ligand in *cis* positions relative to the Os–Os edge [C(22)–Os(2)–Os(3) = 118.0(5)°, P(2)–Os(3)–Os(2) = 117.88(9)°] constitutes further evidence for the location of the hydride. The Os–P distances [Os(3)–P(2) = 2.338(4) and Os(1)–P(1) = 2.314(4) Å] are comparable to those in **2**. It is apparent that compound **3** may be derived from (the *trans–trans* isomer of) **2** by loss of one carbonyl group and subsequent coordination of the thienyl ring. As expected, thermolysis of **2** at 110 °C gave **3** in good yield (65%). In this reaction, there was however no evidence of the formation of a compound involving the above-mentioned triply bridging (axial) coordination mode of the thienylphosphine ligand, i.e. $[Os_3(\mu\text{-H})(CO)_8\{\mu_3\text{-}P(C_4H_2S)(C_4H_3S)_2)\}\{P(C_4H_3S)_3\}]$ (**8**, *vide infra*), the diphenyl(thienyl)phosphine analogue of which is known [12]. It may be that the slightly smaller cone angle of the trithienylphosphine, relative to diphenyl(thienyl)phosphine, permits the former ligand to fit in the equatorial plane of trinuclear metal carbonyl clusters while the latter ligand is too large for such a coordination mode. On the other hand, the triply bridging coordination mode of trithienylphosphine could be detected upon thermolysis of **1** (*vide infra*).

Treatment of $[Os_3(\mu\text{-H})_2(CO)_{10}]$ with one molar equivalent of $P(C_4H_3S)_3$ at room temperature gave $[Os_3(\mu\text{-H})_2(CO)_9\{P(C_4H_3S)_3\}]$ (**5**) and $[Os_3H(\mu\text{-H})(CO)_{10}$-

Table 1
Crystal data and structure refinement for **2**, **3**, **5**, **6** and **7**

	2	**3**	**5**	**6**	**7**
Chemical formula	$C_{34}H_{18}O_{10}Os_3P_2S_6$	$C_{33}H_{18}O_9Os_3P_2S_6$	$C_{21}H_{11}O_9Os_3PS_3$	$C_{22}H_{11}O_{10}Os_3PS_3$	$C_{21}H_9O_9Os_3PS_3$
Formula weight	1411.38	1383.37	1105.05	1133.06	1103.03
Temperature (K)	293(2)	293(2)	293(2)	150(2)	293(2)
Radiation, wavelength (Å)	0.71073	0.71073	0.71073	0.71073	0.71073
Crystal system, space group	Monoclinic, $C2/c$	Monoclinic, $P2_1/c$	Triclinic, $P\bar{1}$	Triclinic, $P\bar{1}$	Triclinic, $P\bar{1}$
Unit cell parameters					
a (Å)	31.572(5)	16.0909(11)	9.3009(6)	9.0860(13)	13.1275(14)
b (Å)	12.5465(16)	11.1466(7)	9.5691(6)	12.4254(18)	13.7810(15)
c (Å)	20.017(3)	22.2224(15)	16.4492(11)	13.2620(19)	17.0252(18)
α (Å)	90	90	98.1810(10)	67.485(2)	113.131(2)
β (°)	90	101.1780(10)	103.0320(10)	82.253(2)	100.378(2)
γ (°)	90	90	94.7520(10)	83.174(2)	102.307(2)
Cell volume (Å^3)	7929.1(18)	3910.2(4)	1401.72(16)	1366.8(3)	2645.3(5)
Z	8	4	2	2	4
Calculated density (g/cm^3)	2.365	2.350	2.618	2.753	2.770
Absorption co-efficient (μmm^{-1})	10.043	10.178	13.890	14.251	14.720
F (000)	5248	2568	1000	1028	1992
Crystal colour and size (mm^3)	Orange, $0.57 \times 0.17 \times 0.12$	Yellow, $0.46 \times 0.28 \times 0.23$	Maroon, $0.40 \times 0.24 \times 0.04$	Yellow, $0.41 \times 0.38 \times 0.16$	Yellow, $0.31 \times 0.17 \times 0.16$
θ Range for data collection (°)	1.75–28.32	2.05–28.31	2.32 to 28.30	2.27 to 28.25	1.63 to 28.31
Index ranges	h −41 to 41, k −16 to 16, l −26 to 26	h −21 to 20, k 0–14, l 0–29	h −12 to 12, k −12 to 12, l −21 to 21	h −11 to 12, k −16 to 16, l −17 to 17	h −17 to 17, k −18 to 17, l −22 to 22
Completeness to $\theta = 28.32°$	59.2%	99.9%	92.8%	98.2%	99.2%
Reflections collected	15792	9327	12449	11559	23355
Independent reflections [R_{int}]	5847 [0.0783]	9327 [0.0000]	6463 [$R_{int} = 0.0337$]	6196 [$R_{int} = 0.0458$]	12176 [$R_{int} = 0.0337$]
Reflections with $F^2 > 2\sigma$	4334	8119	5692	5564	9583
Absorption correction	Semi-empirical from equivalents	Numerical	Semi-empirical from equivalents	Semi-empirical from equivalent	Semi-empirical from equivalents
Minimum and maximum Transmission	0.0693 and 0.3787	0.0891 and 0.2030	0.0713 and 0.5801	0.0676 and 0.2089	0.0920 and 0.2087
Structure solution	Direct methods	Direct methods	Direct methods	Patterson synthesis	Direct methods
Refinement method	Full-matrix least-squares on F^2	Full-matrix least-squares on F^2	Full-matrix least-squares on F^2	Full-matrix least-squares on F^2	Full-matrix least-squares on F^2
Weighting parameters a, b	0.0694, 0.0000	0.0630, 135.3756	0.0555, 2.6987	0.0996, 0.0000	0.0762, 0.0000
Data/restraints/parameters	5847/0/505	9327/0/493	6463/0/404	6196/0/347	12176/4/682
Final R indices [$F^2 > 2\sigma$]	$R_1 = 0.0722$, $wR_2 = 0.1608$	$R_1 = 0.0703$, $wR_2 = 0.1704$	$R_1 = 0.0406$, $wR_2 = 0.1054$	$R_1 = 0.0554$, $wR_2 = 0.1455$	$R_1 = 0.0526$, $wR_2 = 0.1266$
R indices (all data)	$R_1 = 0.0853$, $wR_2 = 0.1650$	$R_1 = 0.0797$, $wR_2 = 0.1761$	$R_1 = 0.0461$, $wR_2 = 0.1089$	$R_1 = 0.0601$, $wR_2 = 0.1504$	$R_1 = 0.0681$, $wR_2 = 0.1349$
Goodness-of-fit on F^2	0.972	1.090	1.048	1.031	1.008
Largest and mean shift/su	0.001 and 0.000	0.000 and 0.000	0.001 and 0.000	0.001 and 0.000	0.001 and 0.000
Largest difference in peak and hole (e Å^{-3})	2.811 and −1.630	13.193 and −3.239	2.222 and −2.738	4.581 and −6.255	3.990 and −2.841

$\{P(C_4H_3S)_3\}]$ (**6**) which were characterized by a combination of spectroscopic data and single crystal X-ray analysis. The carbonyl stretching frequencies in the IR spectrum of **5** are similar to those of $[Os_3(\mu\text{-}H)_2(CO)_9(PPh_3)]$ [22] and $[Os_3(\mu\text{-}H)_2(CO)_9(P^iPr_3)]$ [23], indicating that it is isostructural to these clusters. The ^{1}H NMR spectrum shows three multiplets for the thienyl hydrogens at δ 7.78, 7.35 and 7.27, each integrating for three hydrogens and a doublet at δ −10.18 ($J = 8.1$ Hz) integrating for two hydrogens, i.e. the hydrides. The $^{31}P\{^1H\}$ NMR spectrum displays a singlet at δ −16.53. The FAB mass spectrum confirms the stoichiometry with a molecular ion peak at m/z 1106 and ions formed by successive loss of nine CO groups.

The solid-state molecular structure of **5** is depicted in Fig. 3. Compound **5** has a 46 valence electron count and is thus formally unsaturated. The molecule consists of an isosceles triangle of osmium atoms with two almost equal [Os(1)–Os(3) = 2.814(4) and Os(1)–Os(2) = 2.808(4) Å] and one significantly shorter [Os(2)–Os(3) = 2.684(4) Å] metal–metal bonds, one terminal tris(2-thienyl)phosphine and nine terminal carbonyl ligands. The Os(2)–Os(3) edge is doubly bridged by two hydrides and the tris(2-thienyl)phosphine ligand is coordinated to Os(1) in an

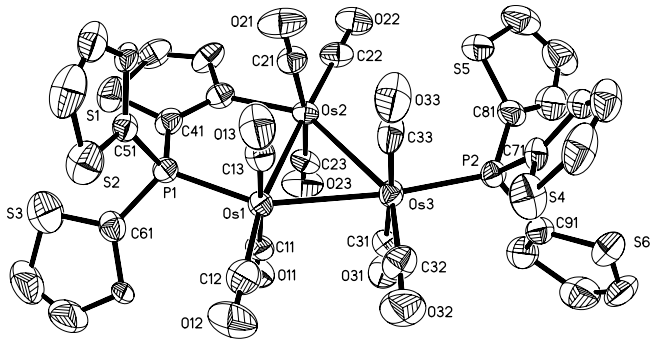

Fig. 2. Solid–state molecular structure of $[Os_3(\mu\text{–}H)(CO)_9\{\mu\text{-}P(C_4H_3S)_2(C_4H_2S)\}\text{–}\{P(C_4H_3S)_3\}]$ (**3**). Thermal ellipsoids are drawn at the 50% probability level. The hydrogen atoms have been omitted for the sake of clarity. Selected bond lengths (Å) and angles (°): Os(1)–Os(2) = 2.8569(7), Os(1)–Os(3) = 2.9102(8), Os(2)–Os(3) = 3.0564(7), Os(2)–C(42) = 2.130(14), Os(1)–P(1) = 2.314(4), Os(1)–P(1) = 2.314(4), S(1)–C(41) = 1.732(15), S(1)–C(44) =1.711(19), C(41)–C(42) = 1.42(2), C(43)–C(44) = 1.35(2), C(42)–C(43) = 1.428(18), Os(2)–Os(1)–Os(3) = 63.999(19), Os(1)–Os(2)–Os(3) = 58.847(18), Os(1)–Os(3)–Os(2) = 57.154 (17), C(42)–Os(2)–Os(1) = 89.1(4),C(22)–Os(2)–Os(3) = 118.0(5), P(1)–Os(1)–Os(2) = 88.20(9), C(31)–Os(3)–Os(2) = 87.4(5),C(41)–P(1)– C(61) = 107.4(7), C(41)–P(1)–Os(1) = 112.2(5), C(31)–Os(3)–P(2) = 95.2(5), P(2)–Os(3)–Os(2) = 117.88(9).

equatorial coordination site. The gross structure of **5** is essentially the same as that of the parent cluster $[Os_3(\mu\text{-}H)_2(CO)_{10}]$ [24], except a tris(2-thienyl)phosphine ligand has been substituted for one of the equatorially positioned carbonyl ligands on one of the hydride bridged osmium atoms. The nine linear terminal carbonyl ligands are distributed in a 4:3:2 pattern as shown in Fig. 3. The Os(2)–Os(3) distance [2.6847(4) Å] is almost identical to that found in the parent $[Os_3(\mu\text{-}H)_2(CO)_{10}]$ cluster [2.681(1) Å] [24] and its phosphine derivatives $[Os_3(\mu\text{-}H)_2(CO)_9(PPh_3)]$ [2.683(2) Å] [25] and $[Os_3(\mu\text{-}H)_2(CO)_9(P^iPr_3)]$ [2.689(1) Å] [23]. This implies that there is very little perturbation of the $Os(\mu\text{-}H)_2Os$ unit on ligand substitution. The Os(1)–Os(3) and Os(1)–Os(2) distances of 2.8146(4) Å and 2.8088(4) Å, respectively, are very similar to the corresponding distances in $[Os_3(\mu\text{-}H)_2(CO)_{10}]$ [2.815 and 2.814 Å] [24] and $[Os_3(\mu\text{-}H)_2(CO)_9(P^iPr_3)]$ [2.816(1) and 2.822(1) Å] [23]. The Os(2)–P(1) bond distance of 2.3272(19) Å in **5** is significantly shorter than that in $[Os_3(\mu\text{-}H)_2(CO)_9(P^iPr_3)]$ [2.384(5) Å] [23] and slightly shorter than that found in $[Os_3(\mu\text{-}H)_2(CO)_9(PMe_2Ph)]$ [2.347(5) Å] [26], indicating that the Os–P bond distances increase with the increase of steric bulk of the phosphine.

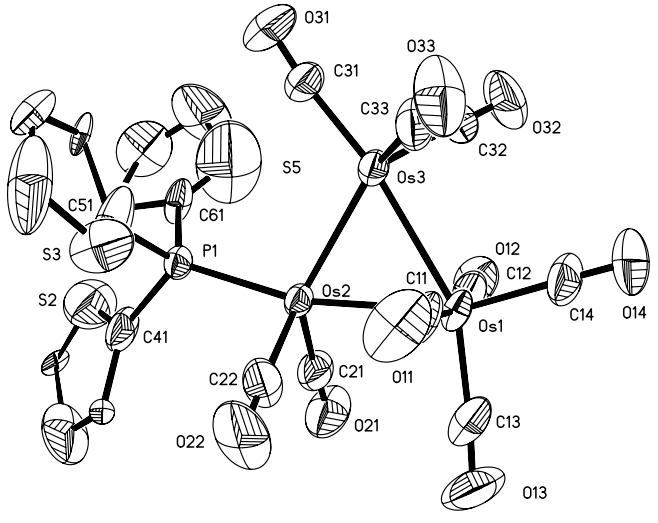

Fig. 3. Solid-state molecular structure of $[Os_3(\mu\text{-}H)_2(CO)_9\{P(C_4H_3S)_3\}]$ (**5**). Thermal ellipsoids are drawn at the 50% probability level. Selected bond lengths (Å) and angles (°): Os(1)–Os(2) = 2.8088(4), Os(1)–Os(3) = 2.8146(4), Os(2)–Os(3) = 2.6847(4), Os(2)–P(1) = 2.3272(19), Os(2)–Os(1)–Os(3) = 57.033(10), Os(3)–Os(2)–Os(1) = 61.593(11), Os(2)–Os(3)–Os(1) = 61.374(11), C(22)–Os(2)–Os(3) = 129.2(4), P(1)–Os(2)–Os(3) = 105.15(5), C(21)–Os(2)–Os(1) = 105.15(5), C(21)–Os(2)–Os(1) = 91.0(3), C(21)–Os(2)–Os(3) = 132.5(3), C(22)–Os(2)–Os(1) = 95.5(3), C(31)–Os(3)–Os(2) = 109.6(3), C(33)–Os(3)–Os(1) = 93.8(3) C(32)–Os(3)–Os(1) = 90.0(3). The figure displays one of the orientations of the thienyl groups of the phosphine ligand (cf. Section 4).

The infrared spectrum of **6** in the carbonyl region is very similar to that of $[Os_3H(\mu\text{-}H)(CO)_{10}(Ph_2PCH{=}CH_2)]$ [27], $[Os_3H(\mu\text{-}H)(CO)_{10}(PPh_3)_2]$ [22] and $[Os_3H(\mu\text{-}H)(CO)_{10}\text{-}\{Ph_2P(C_4H_3S)\}]$ [12] suggesting that it is isostructural to these clusters. The ^1H NMR spectrum of **6** shows multiplets for the thienyl hydrogens at δ 7.75, 7.50 and 7.27, each integrating for three hydrogens, and a broad hydride resonance at δ −14.55 integrating for two hydrogens. The broad hydride resonance implies fluxional behaviour (not investigated) as observed for $[Os_3H\text{-}(\mu\text{-}H)(CO)_{10}(Ph_2PCH{=}CH_2)]$ [27], $[Os_3H(\mu\text{-}H)(CO)_{10}\text{-}\{Ph_2P(C_4H_3S)\}]$ [12] and $[Os_3H(\mu\text{-}H)(CO)_{10}(L)\}]$ (L = PEt_3, $HPEt_2$, H_2PPh, $HPPh_2$) [28]. The $^{31}P\{^1H\}$NMR spectrum contains one singlet at δ −23.0. The FAB mass spectrum of **6** shows molecular ion peak at m/z 1134 which fragmented by loss of 10 CO groups.

The structure proposed for **6** was confirmed by an X-ray diffraction study. The molecular structure of **6** is depicted in Fig. 4. The overall structure of the molecule is very similar to $[Os_3H(\mu\text{-}H)(CO)_{10}(PPh_3)]$ [29], the solid state structure of which has been determined. Cluster **6** consists of an Os_3 triangle involving three distinctly different metal–metal bonds [Os(1)–Os(2) = 2.8709(6), Os(2)–Os(3) = 2.9232(5) and Os(1)–Os(3) = 3.0060(6) Å]. Ten linear carbonyl groups are arranged such that Os(2) has four while the remaining osmium atoms have three each. The average metal–metal bond distance [2.9333(6) Å] is significantly longer than the Os–Os bond distances in the parent cluster $[Os_3(CO)_{12}]$ [2.877(3) Å] [30]. It is possible to predict that the bridging hydride spans the Os(1)–Os(3) edge since this edge is substantially longer than the other two. The tris(2-thienyl)phosphine ligand is in an equatorial coordination site on Os(3) [Os(3)–P(1) = 2.338(2) Å] and is *trans* to the Os–Os vector and *cis* to the bridging hydride. Five isomers of the compound $[Os_3H(\mu\text{-}H)(CO)_{10}(L)\}]$ (L = PEt_3, $HPEt_2$, H_2PPh, $HPPh_2$), which differ in the relative orientation of the coordinated phosphine to the hydrides, have been detected by low temperature NMR spectroscopy [28]. It has also been demonstrated that the kinetically

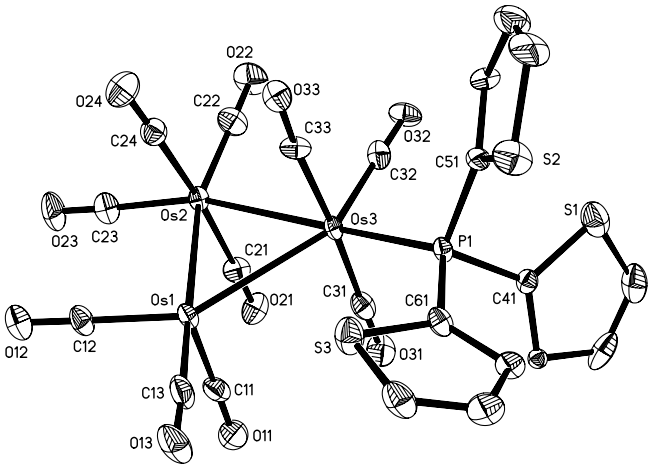

Fig. 4. Solid-state molecular structure of $[Os_3H(\mu\text{-}H)(CO)_{10}\{P(C_4H_3S)_3\}]$ (**6**).Thermal ellipsoids are drawn at the 50% probability level. The hydrogen atoms have been omitted for clarity. Selected bond lengths (Å) and angles (°): Os(1)–Os(2) = 2.8709(6), Os(1)–Os(3) = 3.0060(6), Os(2)–Os(3) = 2.9232(5), Os(3)–P(1) = 2.338(2), Os(1)–Os(2)–Os(3) = 62.498 (14), Os(2)–Os(1)–Os(3) = 59.603(11), Os(2)–Os(3)–Os(1) = 57.899(13), Os(1)–Os(2)–Os(3) = 62.498(14), C(11)–Os(1)–Os(2) = 94.1(3), C(13)–Os(1)–Os(3) = 116.7(3), C(12)–Os(1)–Os(2) = 88.2(3), C(13)–Os(1)–Os(2) = 172.1(3), C(11)–Os(1)–Os(3) = 93.9(3), P(1)–Os(3)–Os(2) = 173.11(6), P(1)–Os(3)–Os(1) = 118.43(5), C(31)–Os(3)–Os(1) = 88.2(3), C(12)–Os(1)–Os(3) = 146.8(3), C(13)–Os(1)–Os(3) = 116.7(3), C(11)–Os(1)–Os(3) = 93.9(3), C(32)–Os(3)–Os(1) = 145.6(3), C(33)–Os(3)–Os(1) = 87.8(3).

favored isomers have the phosphines in an axial position and the most thermodynamically stable isomer has the phosphine in an equatorial position *cis* to the bridging hydride [27,28]. It is reasonable to propose that compound **6** is an intermediate in the formation of **5** [12]. Indeed, a separate experiment showed that thermolysis of **6** in refluxing heptane yields **5** (cf. Section 4).

The reaction of $[Os_3(\mu\text{-}H)_2(CO)_{10}]$ with $P(C_4H_3S)_3$ at elevated temperature (110 °C) afforded **5** and the cyclometallated products $[Os_3(\mu\text{-}H)(CO)_9\{\mu_3\text{-}P(C_4H_2S)(C_4H_3S)_2\}]$ (**7**) and $[Os_3(\mu\text{-}H)(CO)_8\{\mu_3\text{-}P(C_4H_2S)(C_4H_3S)_2\}\{P(C_4H_3S)_3\}]$ (**8**) in 23%, 17% and 21% yields, respectively (Scheme 2). Compound **7** can also be obtained in good yield (85%) from the thermolysis of **1** at 110 °C. The carbonyl absorption bands of **7** are similar to those of $[Os_3(\mu\text{-}H)(CO)_9\{\mu_3\text{-}Ph_2P(C_4H_2S)\}]$ [12], and $[Ru_3(\mu\text{-}H)(CO)_9\{\mu_3\text{-}Ph_2P(C_4H_2S)\}]$ [11], suggesting that they have similar structures. The ^1H NMR spectrum of **7** shows six doublets of doublets of doublets and two doublets of doublets in the aromatic region and a hydride doublet at δ −17.93 (J = 16.0 Hz) consistent with cyclometallation of one of the thienyl rings. The $^{31}P\{^1H\}$ NMR spectrum of **7** shows a singlet at δ −33.03. The mass spectrum of **7** confirms the stoichiometry with a molecular ion peak at m/z 1104.

The molecular structure of **7** is shown in Fig. 5. The molecule consists of an Os_3 triangle with three distinctly different metal–metal bonds [Os(4)–Os(5) = 3.0145(7), Os(5)–Os(6) = 2.7578(6) and Os(4)–Os(6) = 2.8536(6) Å], a triply bridging $P(C_4H_2S)(C_4H_3S)_2$ ligand, a bridging hydride and nine terminal carbonyl ligands. The μ_3-$P(C_4H_2S)(C_4H_3S)_2$ ligand is bonded through the P(2) atom in an axial position to Os(4) [Os(4)–P(2) = 2.339(3)] through a σ–Os(5)–C(84) bond [Os(5)–C(84) = 2.159(11)] and through an η^2 (π)-interaction between C(83), C(84) and Os(6) [Os(6)–C(83) = 2.380(11) and Os(6)–C(84) = 2.333(11) Å], thus forming an σ, η^2-vinyl type bridge between the metal atoms Os(5) and Os(6). The resulting coordination mode (μ–η^1:η^2) of the thienyl fragment is comparable with that observed in $[Ru_3(\mu\text{-}H)(CO)_8\{\mu_3\text{-}Ph_2P(C_4H_2S)\}\{Ph_2P(C_4H_3S)\}]$ for the μ_3-$Ph_2P(C_4H_2S)$ ligand [11]. The location of the hydride could be determined from the electron density map, and the disposition of the hydride on the same edge that is simultaneously bridged by the orthometalated ligand is in agreement with the structures observed for $[Ru_3(\mu\text{-}H)(CO)_9\{\mu_3\text{-}PPh_2(C_8H_4S)\}]$ [11], $[Os_3(\mu\text{-}H)(CO)_9(\mu_3\text{-}Ph_2PCH{=}CH)]$ [27] $[Os_3(\mu\text{-}H)(CO)_8\{\mu_3\text{-}PPh_2(C_4H_3S)\}]$ [12] and $[Os_3(\mu\text{-}H)(CO)_9\{\mu_3\text{-}PMePh(C_6H_4)\}]$ [31]. As in the case of **3**, the orthometallation of the ligand yields a

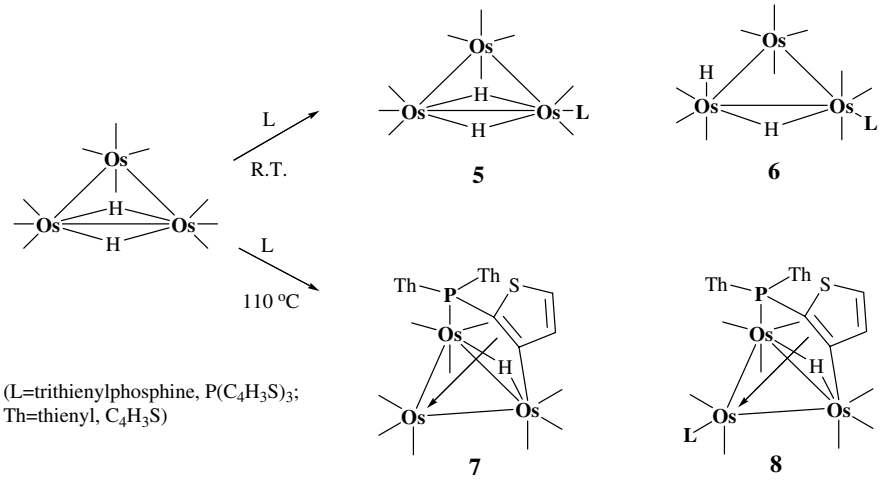

Scheme 2.

chiral cluster framework but the compound crystallizes as a racemate.

The infrared spectrum of **8** is very similar to that of $[Os_3(\mu\text{-}H)(CO)_8\{\mu_3\text{-}Ph_2P(C_4H_2S)\}\{Ph_2P(C_4H_3S)\}]$ [12], indicating that they are isostructural. The ^1H NMR spectrum of **8** shows eight well separated signals for the protons of the μ_3-$P(C_4H_2S)(C_4H_3S)_2$ ligand and three multiplets for the terminally coordinated $P(C_4H_3S)_3$ ligand in addition to the hydride signal at δ −16.98 ppm (dd), indicating that the bridging hydride is coupled to two nonequivalent phosphorus nuclei. As expected, the $^{31}P\{^1H\}$ NMR spectrum displays two doublets at δ −32.15 and −32.88 ($J = 22.2$ Hz). The mass spectrum shows the molecular ion peak at m/z 1356 and ions formed by successive loss of eight CO groups. Compound **8** can be derived from **7** by substitution of one CO ligand by $P(C_4H_3S)_3$ as well as from **3** by removal of one CO ligand followed by coordination of one of the double bonds of the thiophyne (C_4H_2S) ring. As expected, the thermolysis of **3** at 110 °C results in the formation of **8** in high yield. No single crystals of compound **8** suitable for X-ray diffraction could be obtained. Therefore, the structure proposed for this compound (cf. Scheme 2), although support by its analytical and spectroscopic data, could not be unambiguously established.

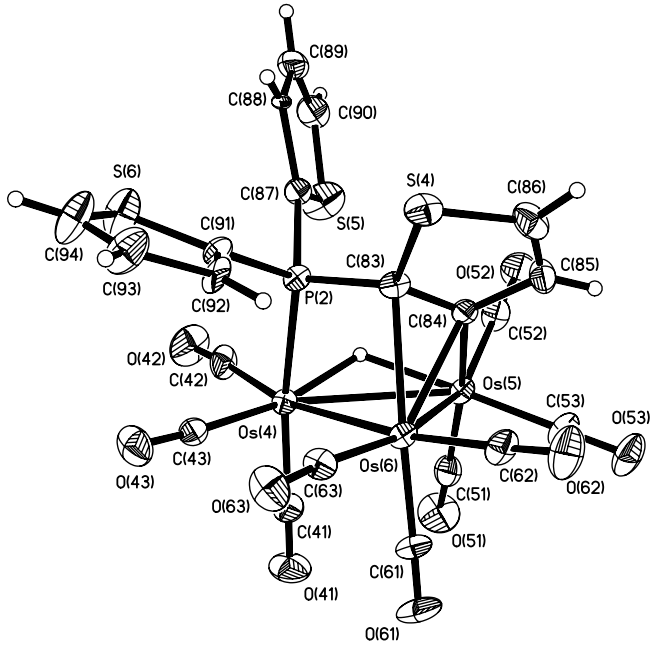

Fig. 5. Solid state molecular structure of $[Os_3(\mu\text{-}H)(CO)_9\{\mu_3\text{-}P(C_4H_2S)(C_4H_3S)_2\}]$ (**7**). Thermal ellipsoids are drawn at the 50% probability level. All hydrogen atoms, except the hydride, have been omitted for the sake of clarity. Selected bond lengths (Å) and angles (°): Os(4)–Os(5) = 3.0145(7), Os(5)–Os(6) = 2.7578(6), Os(4)–Os(6) = 2.8536(6) Å}, Os(4)–P(2) = 2.339(3), Os(5)–C(84) = 2.159(11), S(4)–C(86) = 1.705(15), C(83)–C(84) = 1.391(15), C(85)–C(86) = 1.345(19), Os(6)–Os(4)–Os(5) = 55.984(16), Os(5)–Os(6)–Os(4) = 64.961(17), Os(6)–Os(5)–Os(4) = 59.054(14), P(2)–Os(4)–Os(5) = 85.18(7), P(2)–Os(4)–Os(6) = 74.51(7), C(83)–Os(6)–Os(5) = 76.0(3), C(83)–Os(6)–Os(4) = 77.0 (2), C(84)–Os(5)–Os(6) = 55.1(3), C(84)–Os(6)–Os(4) = 85.6(3), C(84)–Os(5)–Os(4) = 84.8(3), C(83)–Os(6)–Os(5) = 76.0(3), C(42)–Os(4)–Os(5) = 115.7(4), C(52)–Os(5)–Os(4) = 117.7(4).

3. Conclusions

Four triosmium carbonyl compounds, of which $[Os_3(CO)_{11}\{P(C_4H_3S)_3\}]$ (**1**), $[Os_3(CO)_{10}\{P(C_4H_3S)_3\}_2]$ (**2**) and $[Os_3(CO)_9\{P(C_4H_3S)_3\}_3]$ (**4**) are direct phosphine-substitution products and $[Os_3(\mu\text{-}H)(CO)_9\{\mu\text{-}P(C_4H_2S)(C_4H_3S)_2\}\{P(C_4H_3S)_3\}]$ (**3**) is a cyclometallated product, with a previously unknown coordination mode of the thienylphosphine ligand, could be prepared from the reaction between $[Os_3(CO)_{12}]$ and tris-2-thienylphosphine at elevated temperature. The unsaturated cluster $[Os_3(\mu\text{-}H)_2(CO)_{10}]$ reacts with tris(2-thienyl)phosphine at ambient temperature to give the substitution product $[Os_3(\mu\text{-}H)_2(CO)_9\{P(C_4H_3S)_3\}]$ (**5**) as well as the addition product $[Os_3H(\mu\text{-}H)(CO)_{10}\{P(C_4H_3S)_3\}]$ (**6**), whereas at elevated temperature the cyclometallated products $[Os_3(\mu\text{-}H)(CO)_9\{\mu_3\text{-}P(C_4H_2S)(C_4H_3S)_2\}]$ (**7**) and $[Os_3(\mu\text{-}H)(CO)_8\{\mu_3\text{-}P(C_4H_2S)(C_4H_3S)_2\}\{P(C_4H_3S)_3\}]$ (**8**) are obtained in addition to **5**. Cluster **5** is formed from **6** via carbonyl loss as observed for related clusters [12,22,28], indirectly explaining why no formation of **6** could be detected in reactions at elevated temperatures. In compound **3**, the μ-$P(C_4H_2S)(C_4H_3S)_2$ ligand is didentate, i.e. bound through the phosphorus and a carbon atom of the cyclometallated thiophene ring, whereas in both **7** and **8**, the triply bridging $P(C_4H_2S)(C_4H_3S)_2$ ligand is coordinated through the phosphorus and through a μ–η^1:η^2-type interaction of the thienyl group.

4. Experimental

The clusters $[Os_3(\mu\text{-}H)_2(CO)_{10}]$ [32] and $[Os_3(CO)_{11}(MeCN)]$ [33] were synthesized by published methods. Tris(2-thieny)phosphine was purchased from Lancaster and used as received. Solvents were dried by standard methods prior to use. Thin layer chromatography (TLC) separations were performed on commercial plates precoated with Merck Kieselgel 60 to 0.5 mm thickness. NMR spectra were recorded on a Varian Unity 300WB or a Bruker DRX500 spectrometer. Chemical shifts for the $^{31}P\{^1H\}$ NMR spectra are relative to 85% H_3PO_4. IR spectra were recorded on a Nicolet Avatar FT-IR and on a Shimadzu FT-IR spectrophotometer. Elemental analyses were carried out at the microanalytical Laboratories, University College London. FAB mass spectra were recorded on a Jeol SX-102 mass spectrometer using 3-nitrobenzyl alcohol as matrix and CsI as calibrant.

4.1. Reaction of $[Os_3(CO)_{12}]$ with $P(C_4H_3S)_3$

A toluene solution (30 mL) of $[Os_3(CO)_{12}]$ (250 mg, 0.275 mmol) and $P(C_4H_3S)_3$ (108 mg, 0.386 mmol) was heated to reflux for 3.5 h. The solvent was removed under reduced pressure and the residue chromatographed by

TLC on silica gel. Elution with hexane/CH_2Cl_2 (3:2, v/v) gave four bands. The first band gave $[Os_3(CO)_{12}]$ (trace), while the second band afforded $[Os_3(CO)_{11}\{P(C_4H_3S)_3\}]$ (**1**) (90 mg, 28%) as yellow crystals from hexane/CH_2Cl_2 at room temperature. The third band afforded $[Os_3(CO)_{10}\{P(C_4H_3S)_3\}_2]$ (**2**) (130 mg, 33%) as orange crystals and $[Os_3(\mu\text{-}H)(CO)_9\{\mu_3\text{-}P(C_4H_2S)(C_4H_3S)_2\}\{P(C_4H_3S)_3\}]$ (**3**) (50 mg, 13%) as yellow crystals after fractional crystallization from hexane/CH_2Cl_2 at −20 °C. The fourth band gave $[Os_3(CO)_9\{P(C_4H_3S)_3\}_3]$ (**4**) (15 mg, 3%) as orange crystals.

4.2. Spectroscopic and analytical data for 1–4

For **1**: Anal. Calc. for $C_{23}H_9O_{11}Os_3PS_3$: C, 23.83; H, 0.78; P, 2.67. Found: C, 23.54; H, 1.03; P, 2.47%. IR (ν_{CO}, CH_2Cl_2): 2109 m, 2057 vs, 2037 m, 2020 s, 1992 m, 1986 sh, 1967 w cm^{-1}; ^1H NMR ($CDCl_3$): δ 7.69 (m, 3H), 7.40 (m, 3H), 7.25 (m, 3H); $^{31}P\{^1H\}$ NMR: δ −32.97 (s); FAB MS: (*m*/*z*) 1160 (M^+). For**2**: Anal. Calc. for $C_{34}H_{18}O_{10}Os_3P_2S$: C, 28.93; H, 1.29. Found: C, 28.76; H, 1.25%. IR (ν_{CO}, CH_2Cl_2): 2090 m, 2035 s, 2017 m, 2003 vs, 1992 sh, 1974 m cm^{-1}; ^1H NMR ($CDCl_3$): δ 7.66 (m, 6H), 7.44 (m, 6H), 7.24 (m, 6H) ; $^{31}P\{^1H\}$ NMR : δ −44.73 (s, br); FAB MS (*m*/*z*):1412 (M^+). For **3**: Anal. Calc. for $C_{33}H_{18}O_9Os_3P_2S_6$: C, 28.65; H, 1.31. Found: C, 27.95; H, 1.32%. IR (ν_{CO}, C_6H_{12}): 2075 m, 2027 s, 2017 s, 2010 vs, 1990 w, 1970 m, 1958 w cm^{-1}; ^1H NMR ($CDCl_3$): δ 8.11 (m, 1H), 7.95 (m, 1H), 7.85 (m, 3H), 7.58 (m, 1H), 7.35 (d, $J = 5.5$ Hz, 1H) , 7.18 (m, 3H), 7.0 (m, 3m), 6.85 (d, $J = 5.5$ Hz, 1H), 6.58 (m, 1H), 6.42 (m, 1H), −17.15 (dd, $J = 15.9$, 11.4 Hz); $^{31}P\{^1H\}$: δ −33.22 (d, $J = 21.3$ Hz), −34.05 (d, $J = 21.3$ Hz); FAB MS(*m*/*z*): 1384 (M^+). For **4**: Anal. Calc. for $C_{45}H_{27}O_9Os_3P_3S_9$: C, 32.48; H, 1.64; P, 5.58. Found: C, 31.93; H, 2.01; P, 4.78%. IR (ν_{CO}, CH_2Cl_2): 2069 m, 2035 s, 2012 sh, 2004 vs, 1983 vs, 1951 w cm^{-1}; ^1H NMR ($CDCl_3$): δ 7.56 (m, 9H), 7.41 (m, 9H), 7.14 (m, 9H); $^{31}P\{^1H\}$ NMR: δ −47.0 (s, br). FAB MS (*m*/*z*): 1662 (M^+).

4.3. Reaction of $[Os_3(CO)_{11}(MeCN)]$ with $P(C_4H_3S)_3$

A CH_2Cl_2 solution (20 mL) of $[Os_3(CO)_{11}(MeCN)]$ (100 mg, 0.108 mmol) and $P(C_4H_3S)_3$ (30 mg, 0.108 mmol) was stirred at room temperature for 2 h. The solvent was removed under reduced pressure and the residue chromatographed by TLC on silica gel. Elution with hexane-CH_2Cl_2 (3:2, v/v) developed two bands. The faster moving band afforded $[Os_3(CO)_{11}\{P(C_4H_3S)_3\}]$ (**1**) (101 mg, 80%) and the slower moving band gave too little product for complete characterization.

4.4. Reactions of $[Os_3(\mu\text{-}H)_2(CO)_{10}]$ with $P(C_4H_3S)_3$

(a) *At room temperature:* To a CH_2Cl_2 solution (25 mL) of $[Os_3(\mu\text{-}H)_2(CO)_{10}]$ (200 mg, 0.234 mmol) was added $P(C_4H_3S)_3$ (66 mg, 0.234 mmol) at room temperature. The colour of the solution immediately changed from purple to yellow. The reaction mixture was stirred for 15 min and the solvent was removed under reduced pressure. The residue was chromatographed by TLC on silica gel. Elution with hexane–CH_2Cl_2 (7:3, v/v) developed three bands which afforded the following compounds, in order of elution: unconsumed $[Os_3(\mu\text{-}H)_2(CO)_{10}]$, $[Os_3(\mu\text{-}H)_2(CO)_9\{P(C_4H_3S)_3\}]$ (**5**) (27 mg, 10%) as red crystals and $[Os_3H(\mu\text{-}H)(CO)_{10}\{P(C_4H_3S)_3\}]$ (**6**) (120 mg, 45%) as yellow crystals after recrystallization from hexane-CH_2Cl_2 at −20 °C.

Analytical and spectroscopic data for **5** and **6**: For **5**: Anal. Calc. for $C_{21}H_{11}O_9Os_3PS_3$: C, 22.82; H, 1.00. Found: C, 21.94; H, 1.17%. IR (ν_{CO}, CH_2Cl_2): 2094 s, 2056 vs, 2019 m, 2006 s, 1993 m, 1969 w cm^{-1}. ^1H NMR ($CDCl_3$): δ 7.78 (m, 3H), 7.35 (m, 3H), 7.25 (m, 3H), −10.18 (d, $J = 8.1$ Hz, 2H); $^{31}P\{^1H\}$ NMR: δ −16.53 (s). MS (*m*/*z*): 1106 (M^+). For **6**: Anal. Calc. for $C_{22}H_{11}O_{10}Os_3PS_3$: C, 23.32; H, 0.98; P, 2.73. Found: C, 23.37; H, 1.35; P, 2.43%. IR (ν_{CO}, CH_2Cl_2): 2108 m, 2069 s, 2052 s, 2028 vs, 1982 w, 1968 w cm^{-1}. ^1H NMR ($CDCl_3$): δ 7.75 (m, 3H), 7.50 (m, 3H), 7.28 (m, 3H); $^{31}P\{^1H\}$ NMR : δ −23.0 (s). MS (*m*/*z*): 1134 (M^+).

(b) *At 110 °C:* To a toluene solution (20 mL) of $[Os_3(\mu\text{-}H)_2(CO)_{10}]$ (200 mg, 0.234 mmol) was added $P(C_4H_3S)_3$ (66 mg, 0.234 mmol) and the reaction mixture was refluxed for 2.5 h during which time the colour changed from purple to yellow, to green and finally to brown. The solvent was removed under reduced pressure and the residue separated by TLC on silica gel. Elution with hexane/CH_2Cl_2 (3:2, v/v) developed four bands which afforded, in order of elution: $[Os_3(CO)_{12}]$ (trace), $[Os_3(\mu\text{-}H)_2(CO)_9\{P(C_4H_3S)_3\}]$ (**5**) (60 mg, 23%) as red crystals, $[Os_3(\mu\text{-}H)(CO)_9\{\mu_3\text{-}P(C_4H_2S)(C_4H_3S)_2\}]$ (**7**) (45 mg, 17%) and $[Os_3(\mu\text{-}H)(CO)_8\{\mu_3\text{-}P(C_4H_2S)(C_4H_3S)_2\}\{P(C_4H_3S)_3\}]$ (**8**) (67 mg, 21%) as yellow crystals after recrystallization from hexane–CH_2Cl_2 by slow evaporation of the solvents.

Analytical and spectroscopic data for **7** and **8**: For **7**: Anal. Calc. for $C_{21}H_9O_9Os_3PS_3$: C, 22.86; H, 0.82; P, 2.81. Found: C, 22.99; H, 0.95; P, 2.65%. IR (ν_{CO}, CH_2Cl_2): 2088 s, 2055 vs, 2032 s, 2014 vs, 1990 m, 1973 sh cm^{-1}; ^1H NMR ($CDCl_3$): δ 7.93 (ddd, 1H, $J = 5.0$, 4.0, 1.0 Hz), 7.83 (ddd, 1H, $J = 5.0$, 43.5, 1.5 Hz, 1H), 7.58 (ddd, 1H, $J = 4.0$, 3.0, 1.0 Hz, 1 H), 7.35 (ddd, $J = 5.0$, 3.5, 1.5 Hz, 1H), 7.32 (dd, $J = 5.5$, 1.0 Hz, 1H), 7.28 (dd, $J = 5.0$, 1.0 Hz, 1H), 7.05 (ddd, $J = 5.0$, 4.0, 1.5 Hz, 1H), 6.98 (ddd, $J = 5.0$, 4.0, 1.5 Hz,1H), −17.93 (d, $J = 15.0$ Hz, 1H); $^{31}P\{^1H\}$ NMR: δ −32.30 (s); FAB MS (*m*/*z*): 1104 (M^+). For **8**: Anal. Calc. for $C_{32}H_{18}O_8Os_3P_2S_6$: C, 28.35; H, 1.34; P, 4.57. Found: C, 29.0; H, 1.69; P, 4.01%. IR (ν_{CO}, CH_2Cl_2): 2075 vs, 2031 s, 2012 s, 1992 w, 1981 w, 1958 m cm^{-1}; ^1H NMR ($CDCl_3$): δ 8.15 (m, 1H), 7.92 (m, 1H), 7.75 (m, 1H), 7.62 (m, 1H), 7.45 (m, 1H), 7.32 (d, $J = 5.5$ Hz, 1H), 7.24 (m, 3H), 7.0 (m, 3H), 6.85 (d, $J = 5.5$ Hz, 1H), 6.70 (m, 3H), 6.58 (m, 1H), −16.98 (dd, $J = 15.75$, 11.50 Hz, 1H); $^{31}P\{^1H\}$ NMR ($CDCl_3$): δ

−32.15 (d, $J = 22.2$ Hz), −32.88 (d, $J = 22.2$ Hz); FAB MS (m/z): 1356 (M^+).

4.4.1. Conversion of $[Os_3(\mu\text{-}H)(CO)_9\{\mu_3\text{-}P(C_4H_2S)(C_4H_3S)_2\}\{P(C_4H_3S)_3\}]$ (3) to $[Os_3(\mu\text{-}H)(CO)_8\{\mu_3\text{-}P(C_4H_2S)(C_4H_3S)_2\}\{P(C_4H_3S)_3\}]$ (8)

A toluene solution (15 ml) of **3** (60 mg, 0.043 mmol) was refluxed for 4 h. The removal of solvent under reduced pressure followed by a similar chromatographic separation to that above gave two bands. The faster moving band gave **8** (49 mg, 85%) and the slower moving band gave unconsumed **3** (trace).

4.4.2. Conversion of $[Os_3(CO)_{11}\{P(C_4H_3S)_3\}]$ (1) to $[Os_3(\mu\text{-}H)(CO)_9\{\mu_3\text{-}P(C_4H_2S)(C_4H_3S)_2\}]$ (7)

A toluene solution (30 mL) of **1** (105 mg, 0.091 mmol) was refluxed for 3 h. A similar work up to that above gave two bands. The faster moving band gave **7** (49 mg, 85%) and the slower moving band gave unconsumed **1** (trace).

4.4.3. Conversion of $[Os_3(CO)_{10}\{P(C_4H_3S)_3\}_2]$ (2) to $[Os_3(\mu\text{-}H)(CO)_9\{\mu_3\text{-}P(C_4H_2S)(C_4H_3S)_2\}\{P(C_4H_3S)_3\}]$ (3)

A thermolysis of **2** (120 mg, 0.085 mmol) similar to that above followed by similar work up gave **3** (87 mg, 75%).

4.4.4. Conversion of $[Os_3H(\mu\text{-}H)(CO)_{10}\{P(C_4H_3S)_3\}]$ (6) to $[Os_3(\mu\text{-}H)_2(CO)_9\{P(C_4H_3S)_3\}]$ (5)

A heptane solution (30 mL) of **6** (27 mg, 0.024 mmol) was heated to reflux for 1 h. The solvent was removed under reduced pressure and the resultant residue was subjected to thin layer chromatography as described above to give one major and three very minor bands. The major band afforded **5** (18 mg, 69%). The yields of the minor bands were too small for complete characterization.

4.4.5. X-ray crystallography

Single crystals of compounds **2**, **3**, **5**, **6** and **7** were mounted on glass fibers and all geometric and intensity data were obtained on a Bruker SMART APEX CCD diffractometer using Mo Kα radiation ($\lambda = 0.71073$ Å) at 150 ± 2 K. Data reduction and integration was carried out with SAINT+ and absorption corrections were applied using the program SADABS [34]. The structures were solved by direct methods and refined using difference-Fourier synthesis. The SHELXTL PLUS V6.10 program package [35] was used for structure solution and refinement. All non-hydrogen atoms were refined on F^2 by full-matrix least-squares using all unique data. Hydrogen atoms, except that bonded to Os, were placed in calculated positions and their thermal parameters linked to those of the atoms to which they were attached (riding model). In the case of **7**, the hydrogen atom bridging Os atoms was located and its positions refined using fixed isotropic thermal parameters. The crystals of compound **3** that were used for the diffraction study were relatively large and had a large mosaic spread. The fully refined structure of **3** contains one ghost peak close to Os(2) due to unresolved problems associated with absorption effects in the large crystal used for the data collection. One of the thienyl rings in **5** was disordered over two sets of orientations, each 50% populated. The crystal data, details of data collection and refinement results are summarized in Table 1.

5. Supplementary material

CCDC 624701, 624702, 624703, 624704 and 624705 contain the supplementary crystallographic data for **2**, **3**, **5**, **6**, and **7**. These data can be obtained free of charge via http://www.ccdc.cam.ac.uk/conts/retrieving.html, or from the Cambridge Crystallographic Data Centre, 12 Union Road, Cambridge CB2 1EZ, UK; fax: (+44) 1223-336-033; or e-mail: deposit@ccdc.cam.ac.uk.

Acknowledgements

This research has been funded by the Swedish Research Council (VR) and the Royal Swedish Academy of Sciences. S.E.K. acknowledges the Royal Society (London) for a fellowship to work at University College London, and thanks the Department of Chemistry, Jahangirnagar University, for a sabbatical leave. M.A.M. acknowledges the Ministry of Education, the Government of the People's Republic of Bangladesh, for study leave.

References

[1] (a) R.J. Angelici, in: R.B. King (Ed.), Encyclopedia of Inorganic Chemistry, vol. 3, Wiley, New York, 1994, pp. 1433–1443;
(b) M.A. Reynolds, I.A. Guzei, R.J. Angelici, J. Chem. Soc., Chem. Commun. (2000) 513;
(c) M.A. Reynolds, I.A. Guzei, R.J. Angelici, Inorg. Chem. 42 (2003) 2191;
(d) M.A. Reynolds, I.A. Guzei, R.J. Angelici, Organometallics 20 (2001) 1071;
(e) J. Chen, R.J. Angelici, Organometallics 18 (1999) 5721;
(f) R. Prins, V.H.J. De Beer, G.A. Somorjai, Catal. Rev-Sci. Eng. 31 (1989) 1;
(g) H. Topsøe, B.S. Clausen, F.E. Massoth, in: J.R. Anderson, M. Boudart (Eds.), Hydrotreating Catalysis: Science and Technology, Springer, Verlag, 1996 (h).
[2] H.D. Kaesz, R.B. King, T.A. Manuel, L.D. Nichols, F.G.A. Stone, J. Am. Chem. Soc. 82 (1960) 4749.
[3] (a) R.B. King, P.M. Treichel, F.G.A. Stone, J. Am. Chem. Soc. 83 (1961) 3600;
(b) R.B. King, F.G.A. Stone, J. Am. Chem. Soc. 82 (1960) 4557.
[4] A.E. Ogilvy, M. Draganjac, T.B. Rauchfuss, S.R. Wilson, Organometallics 7 (1988) 1171.
[5] A.J. Arce, P. Arrojo, A.J. Deeming Y. De Sanctis, J. Chem. Soc., Dalton Trans. (1992) 2423.
[6] A.J. Arce, J. Manzur, M. Marquez, Y. De Sanctis, A.J. Deeming, J. Organomet. Chem. 412 (1991) 177.
[7] A.J. Arce, A.J. Deeming, Y. De Sanctis, R. Marchado, J. Manzur, C. Rivas, J. Chem. Soc., Chem. Commun. (1990) 1568.
[8] A.J. Arce, A. Karam, Y. De Sanctis, M.V. Capparelli, A.J. Deeming, Inorg. Chim. Acta 285 (1999) 277.
[9] J.D. King, M. Monari, E. Nordlander, J. Organomet. Chem. 573 (1999) 272.

[10] A.J. Deeming, M.K. Shinhmar, A.J. Arce, Y. De Sanctis, J. Chem. Soc., Dalton Trans. (1999) 1153.
[11] A.J. Deeming, S.N. Jayasuriya, A.J. Arce, Y. De Sanctis, Organometallics 15 (1996) 786.
[12] N.K. Kiriakidou Kazemifar, M.J. Stchedroff, M. Abdul Mottalib, S. Selva, M. Monari, E. Nordlander, Eur. J. Inorg. Chem. (2006) 2058.
[13] U. Bodensiek, H. Vahrenkamp, G. Rheinwald, H. Stoeckli-Evans, J. Organomet. Chem. 488 (1995) 85.
[14] (a) M.I. Bruce, B.K. Nicholson, M.L. Williams, J. Organomet. Chem. 243 (1983) 69;
(b) M.I. Bruce, J.G. Matisons, B.K. Nicholson, J. Organomet. Chem. 247 (1983) 321;
(c) M.I. Bruce, M.L. Williams, B.K. Nicholson, J. Organomet. Chem. 258 (1983) 63;
(d) K. Biradha, V.M. Hansen, W.K. Leong, R.K. Pomeroy, M.J. Zaworotko, J. Cluster Sci. 11 (2000) 285.
[15] A.J. Deeming, S. Donovan-Mtunzi, S.E. Kabir, P.J. Manning, J. Chem. Soc, Dalton Trans. (1985) 1037.
[16] R.F. Alex, R.K. Pomeroy, Organometallics 6 (1987) 2437.
[17] M.I. Bruce, M.J. Liddell, C.A. Hughes, J.M. Patrick, B.W. Skelton, A.H. White, J. Organomet. Chem. 347 (1988) 157.
[18] W.K. Leong, Y. Liu, J. Organomet. Chem. 584 (1999) 174.
[19] M.I. Bruce, M.J. Liddell, C.A. Hughes, B.W. Skelton, A.H. White, J. Organomet. Chem. 347 (1988) 181.
[20] N.K. Kiriakidou Kazemifar, Ph.D. Thesis. Lund University, 2002.
[21] S.P. Tunik, I.O. Koshevoy, A.J. Poe, D.H. Farrar, E. Nordlander, T.A. Pakkanen, M. Haukka, J. Chem. Soc., Dalton Trans. (2003) 2457.
[22] (a) A.J. Deeming, S. Hasso, J. Organomet. Chem. 88 (1975) C21;
(b) A.J. Deeming, S. Hasso, J. Organomet. Chem. 114 (1976) 313.
[23] L.J. Farrugia, J. Organomet. Chem. 394 (1990) 515.
[24] R.E. Benfield, B.F.G. Johnson, J. Lewis, P.R. Raithby, C. Zuccaro, K. Hendrick, Acta Crystallogr., Sect. B 35 (1979) 2210.
[25] A.J. Deeming, S. Hasso, J. Organomet. Chem. 114 (1976) 313.
[26] M.R. Churchill, F.J. Hollander, J.P. Hutchinson, Inorg. Chem. 16 (1977).
[27] B.F.G. Johnson, J. Lewis, E. Nordlander, P.R. Raithby, J. Chem. Soc., Dalton Trans. (1996) 3825.
[28] S. Aime, R. Gobetto, E. Valls, Inorg. Chim. Acta 275–276 (1998) 521.
[29] R.D. Adams, B.E. Segmuller, Cryst. Struct. Commun. 11 (1982) 1971, 2697.
[30] M.R. Churchill, B.G. DeBoer, Inorg. Chem. 16 (1977) 878.
[31] A.J. Deeming, S.E. Kabir, N.J. Powell, P.A. Bates, M.B. Hursthouse, J. Chem. Soc. Dalton Trans. (1987) 1529.
[32] H.D. Kaesz, Inorg. Synth. 28 (1989) 238.
[33] B.F.G. Johnson, J. Lewis, D.A. Pippard, J. Chem. Soc., Dalton Trans. (1981) 407.
[34] SMART and SAINT Software for CCD Diffractometers, Version 6.1, Bruker AXS, Madison, WI, 2000.
[35] G.M. Sheldrick, University of Göttingen, Germany, 1977.